01 Jan 1996

Comparison of Trickle-Bed and Upflow Reactor Performance at High Pressure: Model Predictions and Experimental Observations

M. R. Khadilkar

Y. X. Wu

M. (Muthanna) H. Al-Dahhan
Missouri University of Science and Technology, aldahhanm@mst.edu

M. P. Dudukovic

et. al. For a complete list of authors, see https://scholarsmine.mst.edu/che_bioeng_facwork/1390

Recommended Citation

Pergamon

S0009-2509(96)00071-1

COMPARISON OF TRICKLE-BED AND UPFLOW REACTOR PERFORMANCE AT HIGH PRESSURE:
MODEL PREDICTIONS AND EXPERIMENTAL OBSERVATIONS

M. R. KHADILKAR, Y. X. WU, M. H. AL-DAHHAN, M. P. DUDUKOVIĆ
Chemical Reaction Engineering Laboratory (CREL)
Campus Box 1198, Washington University, St. Louis, MO 63130, U.S.A.
and
M. COLAKYAN
Union Carbide Corporation
PO. Box 8361, South Charleston, WV 25303, USA

ABSTRACT-Comparison of laboratory trickle-bed and up-flow reactors over a range of operating conditions, which cover both gas and liquid reactant limitations, has been investigated using hydrogenation of alpha-methylstyrene to cumene in a hexane solvent over 2.5% Pd on alumina extrudate catalyst as a test reaction. The results show that when the reaction is gas limited at low pressure and high liquid feed concentration, trickle bed reactor outperforms the upflow reactor. At high pressure and low liquid feed concentration, the reaction becomes liquid limited and upflow reactor performs better. It is concluded that the advantage of upflow or downflow depends on the reaction system type (i.e. whether the reaction is liquid or gas limited). A single criterion for identifying the limiting reactant is proposed which can explain most of the data reported in the literature on these reactors. Comparison of the experimental observations and the predictions of the reactor scale and pellet scale models available in the literature is presented.

INTRODUCTION

Trickle-bed reactors are fixed beds of catalyst contacted by cocurrent downflow of gas and liquid, whereas in upflow reactors (packed bubble columns) the two phases are in cocurrent upflow. Trickle-bed reactors are used widely in industrial practice and are usually operated at high pressures, while upflow reactors are used less frequently on industrial scale but find usage in laboratory scale studies for testing catalyst and alternative feed stocks for commercial trickle-bed processes. Upflow reactors are often preferred in laboratory studies since in them complete wetting can be achieved, while in trickle beds incomplete catalyst wetting has to be accounted for. The reaction rate over externally incompletely wetted packing can be greater or smaller than the rate observed over completely wetted packing. This depends on whether the limiting reactant is present only in the liquid phase or gas phase or in both liquid and gas phases. Some degree of partial wetting may be encountered in industrial units which affects performance. In laboratory reactors, it is not always possible to obtain wetting conditions representative of industrial reactors if same LHSV (liquid hourly space velocity) is used (lower mass velocities lead to partial wetting). The use of upflow at these LHSV's to get fully wetted conditions would yield a different performance depending upon which reactant is limiting. Thus, the difficulties associated with the scale-up of these reactors are mainly due to interactions between the gas, the liquid, and the solid catalyst phase; these interactions being strongly dependent on the reacting system used.

No study has been reported which compares the performance of downflow and upflow modes over a wide range of operating conditions, particularly reactor pressure, and which relates the observed performance to the type of reaction system used (gas-limited or liquid-limited). The few studies that have been reported in the open literature (Goto and Mabuchi, 1984; Beaudry et al., 1987; Mazzarino et al., 1989; Goto et al., 1993) present diverse conclusions regarding the preferred mode of operation (Table 1). Therefore, an extensive study of the effect of the operating conditions on the performance of these reactors is necessary to understand the interplay between performance and various factors affecting it, and to explain why one mode of operation may be better than the other. El-Hisnawi (1981), Beaudry et al. (1987), and Harold and Watson (1993) have proposed models to predict the performance of trickle-bed and /or upflow reactors. El-Hisnawi's model (1981) is based on a reactor scale plug flow model while Beaudry's (1987) and Harold and Watson's (1993) models are based on a pellet scale model. Although these models have been tested for a gas limited reaction system at atmospheric pressure and work well, they have not been tested with regard to the type of the reaction system (gas or liquid limited) for a wide range of operating conditions (high pressure, feed concentration, etc.).

In this study we compare laboratory trickle-bed and upflow reactors over a range of operating conditions which cover both gas and liquid limited conditions using hydrogenation of α-methylstyrene to cumene in n-hexane solvent over 2.5% Pd on alumina extrudate catalyst as a test reaction. This reaction has been used widely as a test reaction in trickle bed reactor studies at atmospheric pressure (Satterfield et al., 1968; Germain et al., 1974; Herskowitz et al., 1979; El-Hisnawi, 1981; Ahn et al., 1986; Chen et al., 1986; Beaudry et al., 1987) due to its advantage of giving a single product and being irreversible. All the reaction rate studies for this reaction have been performed under atmospheric pressure. El-Hisnawi (1981) and Beaudry et al. (1987) found that the reaction is gas limited at high alpha-methylstyrene feed concentration and the observed reaction rate was zero order with respect to alpha-methylstyrene and first order with respect to hydrogen. No study has investigated the reaction rate at high pressure (at increased solubility of hydrogen in n-hexane) and at low feed concentration of the liquid reactant to find out whether at such conditions the reaction would shift toward liquid limitations. Since the prediction of

reactor performance needs kinetic data, it is necessary to investigate the reaction rate of this reaction in order to use the proper rate and effectiveness factor at the operating conditions employed(high pressure and low concentration).

CRITERION FOR GAS/LIQUID LIMITED REACTION

In the present study, and in case of all systems where the rate is not limited by external transport of either reactant, the limiting reactant can be identified by comparing the effective diffusivity terms with the observed rate. This is done by evaluation of the Weisz modulus ($\phi_{We}= (r_A)_{obs}(V_p/S_x)^2/(D_eC)$), where D_eC is the smaller of the two, $D_{eB}C_{Bi}/b$ or $D_{eA}C_A^*$ for the reaction: A+bB→P, where A is hydrogen, B is alpha-methylstyrene and P is cumene, which for our reaction system yields $\phi_{We} > 1$. In order to identify the limiting reactant in case of $\phi_{We} > 1$, the diffusion fluxes of the two reactants should be compared, whereas for $\phi_{We} < 1$, it is the ratio of the liquid reactant concentration and the gas reactant dissolved concentration that counts. Thus, the limiting reactant can be identified by evaluation of the D_eC terms and examining the ratio of this product (effective diffusivities and concentration) for both reacting species in the range of operating conditions of interest (Doraiswamy and Sharma, 1984; Beaudry et al., 1987). This ratio ($\gamma = (D_{eB} C_{Bi}) /b(D_{eA} C_A^*))$ is indicative of the relative availability of the species at the reaction site. A value of $\gamma >> 1$ would imply a gaseous reactant limitation while $\gamma << 1$ indicates liquid reactant limitation. Table 1 lists the calculated γ values for literature and present study.

EXPERIMENTAL

The high pressure packed bed reactor facility used in this study consists of four main components which are: the reactor section, the gas-liquid distributor (for trickle bed operation), the gas distributor (for upflow operation) and the gas-liquid separator as shown in Figure 1 (for a more detailed description, see Al-Dahhan and Dudukovic, 1995). The same bed of catalyst was used (once it was activated and packed) for both modes of operation. For trickle bed reactor operation, all the valves are set to position #1, while for upflow operation all the valves were set to position #2 (Figure 1).
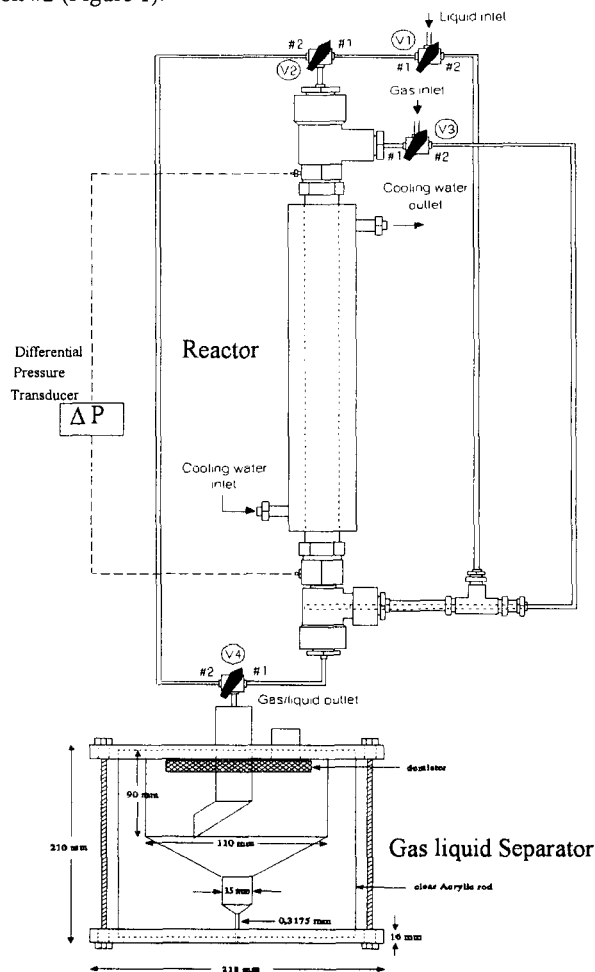

Figure 1: Experimental Setup

The catalyst (2.5% Pd on alumina extrudates) was packed to a height of 0.275 m along with glass beads (3×10^{-3} m diameter) packed on both ends of the column to a total reactor length of 0.5 m. α-methylstyrene (99.9% purity) in hexane (ACS grade, 99.9% purity) was used as the liquid phase and delivered to the reactor by a pre-calibrated high pressure pump. Pure hydrogen (pre-purified, analytical grade) bubbled through a hexane saturator (to prevent evaporation of hexane in the reactor) was used as the gas phase. The reactor was kept isothermal at room temperature (24°C) by a cooling jacket, temperature was readily controlled due to a dilute liquid reactant. Liquid samples were drawn from the gas-liquid separator after steady state was reached at each liquid flow rate. The samples were analyzed by gas chromatography (Gow Mac Series 550, with thermal conductivity detector) from which the conversion of α-methylstyrene was determined. Experiments were conducted at a fixed gas flow rate by varying liquid flow rate for each mode of operation. The stability of the catalyst over the duration of the experiments was verified by taking intermittent samples at identical operating conditions. The reproducibility of the data was observed to be within 3%. The range of operating conditions investigated in this study is presented in Table 2. An autoclave reactor (1 liter size) was used for intrinsic rate (slurry) studies and a basket reactor was used for apparent rate investigations (Wu and Khadilkar, 1995).

INTRINSIC RATE AT HIGH PRESSURE

Before any trickle bed model predictions can be attempted, intrinsic rate and apparent rate data must be obtained. This was the motivation for slurry and basket reactor experiments at high pressure.

The reaction rate in slurry reactors at different pressures and over a range of initial liquid reactant concentrations was investigated. Slurry reactions at low pressure (30 psig) showed the expected dependence (El-Hisnawi et. al, 1981) of zero order with respect to α-methylstyrene. Sufficient agitation was maintained to ensure no external transport limitations in the system, along with a supply of fresh hydrogen to replace whatever was consumed and, hence, saturation concentration of hydrogen in the liquid phase was achieved. A peculiar behavior, encountered sometimes only at very high pressure (>1000 psig), was observed in our high pressure experiments (max. pressure 300 psig) as shown in Figure 2.
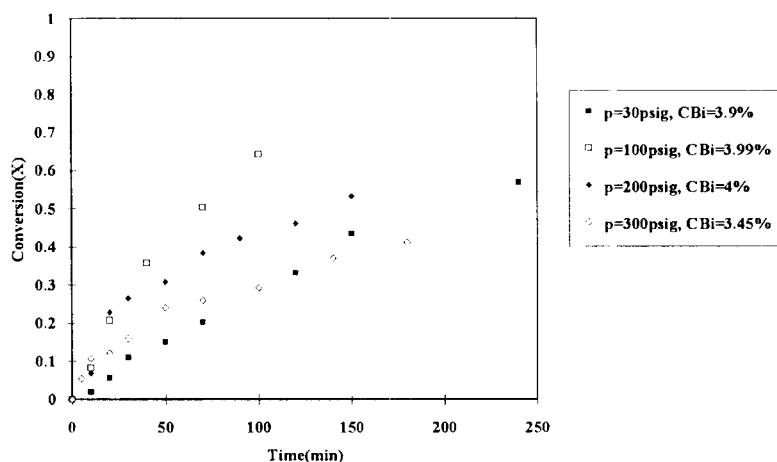

Figure 2: Slurry conversion versus time at different pressures

The rate for a system with approximately the same liquid reactant concentration increased when pressure was raised from 30 to 100 psig but decreased when pressure was increased further from 100 to 200 and 300 psig. This was further augmented by the slight inhibiting effect observed at high pressure which could be attributed due to the presence of cumene, particularly at higher conversions when 8-10% (volume cumene/volume liquid solution) cumene is present in the system. This pressure dependence, and product inhibition, have been observed at a few thousand psig in commercial hydrogenation and hydrodesulphurizations (Satterfield and Roberts, 1968). We first tried to fit the data at all pressure with a single rate form mechanism. Different single and dual site adsorption-reaction mechanisms were tried by considering a shift in the rate limiting step. No simple mechanism was capable of representing this reaction at all pressures, and since our primary objective was to study and predict trickle bed and upflow performance, separate fits were used at each pressure for the general Langmuir-Hinshelwood rate expression (Equation 1). The effect of hydrogen pressure was lumped in the numerator in the rate constant and the adsorption equilibrium constants were obtained by a constrained non-linear fit to at least 30 points of data at each pressure. The fitted parameters at different pressures are presented in Table 3.

$$r = \frac{k_{vs}C_{ams}C_{h2}}{(1+K_1C_{ams}+K_2C_{cume})^\beta} \qquad (1)$$

Since the pellet effectiveness factor was also needed to compare the prediction of the suggested models and experimental observations, the reaction rate in a basket reactor (apparent rate) at different pressures and initial concentrations were investigated also to evaluate the effectiveness factor at each operating condition (Wu and Khadilkar, 1995).

RESULTS AND DISCUSSION
Comparison of Upflow and Downflow Reactors at Gas and Liquid Limited Conditions

Comparison of the two reactors is achieved by studying the conversion at identical volumetric nominal space times (defined as reactor length/ superficial liquid velocity) and identical reactant feed concentration. This is the proper scale-up variable, (space time = 3600/LHSV) when the beds for upflow and downflow are identically packed (i.e. bed voidage = constant). At low pressure (30 psig) and high feed concentration of α-methylstyrene (C_{Bi}= 7.8 %v/v), the reaction is gas limited (γ = 8.8). In this case downflow performs better than upflow reactor as shown in Figure 3.
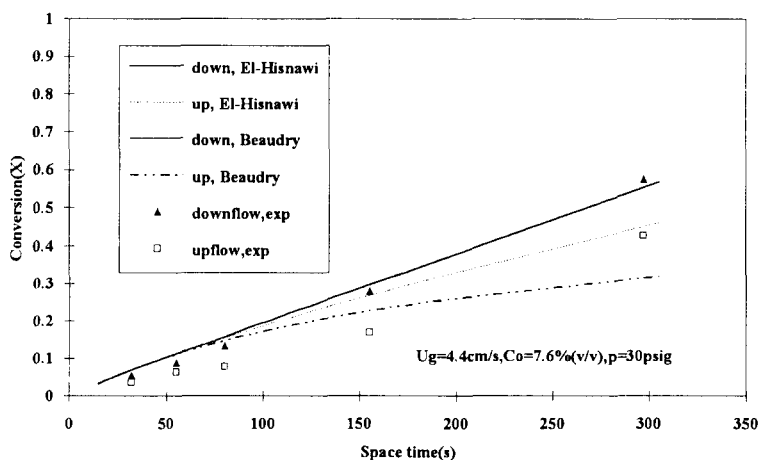

Figure 3: Upflow and Downflow Performance at Low Pressure (gas limited condition): Experimental data and model predictions

This is due to the nature of the hydrogenation reactions which are typically hydrogen (gas reactant) limited at low pressure (at or just above atmospheric) and high α-methylstyrene concentrations (this study, and Beaudry et al., 1987). It is obvious that this is due to low hydrogen solubility at these pressures. In downflow mode of operation, the catalyst particles are not fully wetted at the liquid flow rates used (contacting efficiency < 1) (Al-Dahhan and Dudukovic, 1995). This facilitates the access of the gas reactant to the pores of the catalyst on the externally dry parts and reduces the extent of gas limitation compared to fully wetted pellets in the upflow reactor. The result is a higher conversion in downflow than in the upflow mode of operation. In case of upflow, since the catalyst is almost completely wetted, the access of gaseous reactant to the catalyst site is limited to that through liquid film only. This provides an additional resistance for the gaseous reactant, this effect is increased at high space times due to low gas-liquid mass transfer coefficient and results in conversion lower than that obtained in downflow.
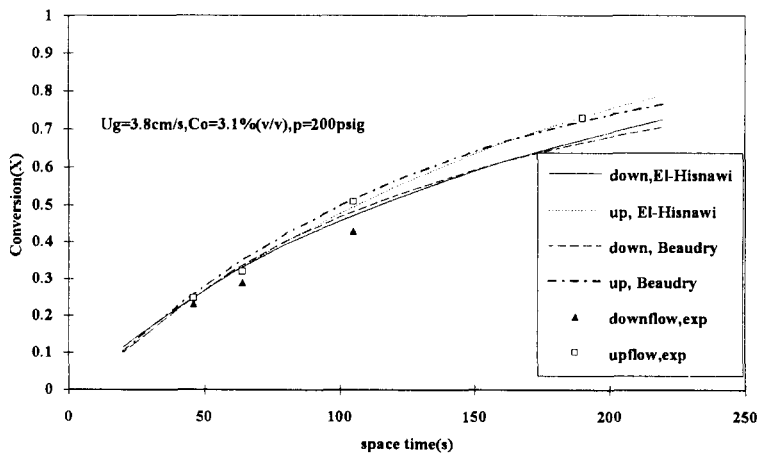

Figure 4: Upflow and Downflow Performance at High Pressure (liquid limited condition): Experimental data and model predictions

This effect is more prominent at higher liquid reactant feed concentrations due to the larger extent of gas limitation (especially at low pressures) where such conditions yield higher γ values. As liquid mass velocity increases (space time decreases) the downflow performance approaches that of upflow due to catalyst wetting efficiency approaching that of upflow (contacting efficiency approaches 1). As the reactor pressure increases and the feed concentration of α-methylstyrene decreases, the value of γ decreases and the reaction approaches liquid limited behavior as mentioned earlier. This is reflected in a complete reversal in performance at higher pressures at low α-methylstyrene concentration (Figure 4) where upflow performs better than downflow. The reason for this is that under these conditions the catalyst in downflow is still partially wetted (since at our operating gas velocities and gas densities (hydrogen), high pressure only slightly improves wetting in downflow (Al-Dahhan and Dudukovic, 1995) while we could assume fully wetted catalyst in upflow. In a liquid limited reaction, the conversion will be governed by the degree of catalyst wetting and since upflow has higher wetting (100 %) than downflow, it will outperform downflow. As the liquid mass velocity increases, and the contacting efficiency of downflow approaches 100 %, the performance of the two reactors approaches each other as evident in Figure 3 and 4. Thus, as pressure is increased from 30 to 200 psig, and feed concentration of α-methylstyrene is decreased from 7.8% to 3.1% (v/v), the reaction is transformed from a gas-limited (γ=8.8) to a liquid-limited regime (γ=0.8).

Effect of feed concentration on performance is shown in Figure 5 (a) and (b). Atmospheric pressure
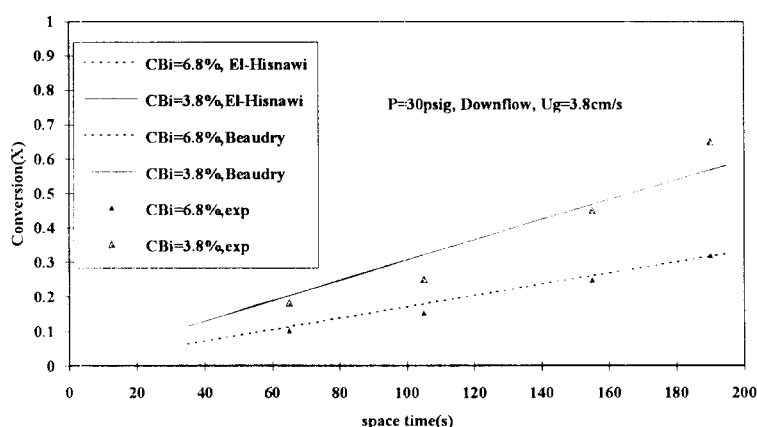
Figure 5 (a): Effect of Feed Concentration on Performance (Downflow)
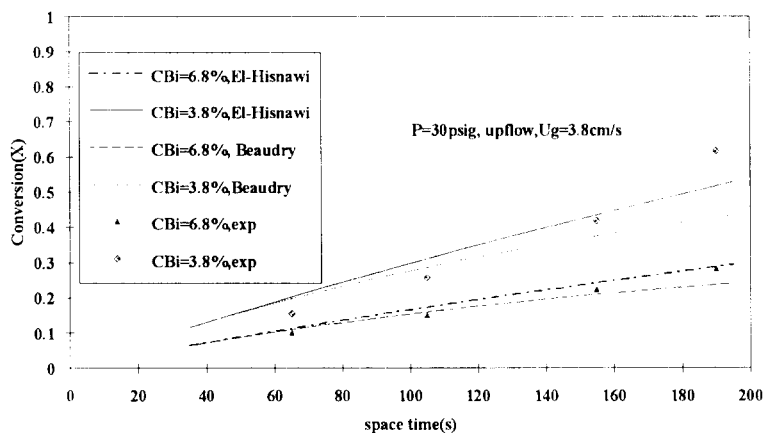
Figure 5 (b): Effect of Feed Concentration on Performance (Upflow)

hydrogenation of alpha-methylstyrene has been known to be a zero order reaction with respect to alpha-methylstyrene and first order with respect to hydrogen (El-Hisnawi, 1981). This study confirms that at 30 psig, the reaction is zero order with respect to alpha-methylstyrene concentration as shown in Figure 5. The conversion is almost independent of feed concentration at further higher pressures (under liquid limited conditions).

Model Predictions of Trickle Bed and Upflow Performance at Different Pressures

The qualitative analysis and arguments made in the previous discussion were quantitatively confirmed using two types of models, a reactor scale heterogeneous plug flow model (El-Hisnawi et al., 1982, see Appendix 1) and a pellet scale model (Beaudry et al., 1987, see Appendix 2). The reactor scale model allows for different rates

on the dry and wetted pellets by considering gas-solid and gas-liquid-solid mass transport along with the pertinent kinetics, which demands numerical solution due to non-linearity of the rate equation, especially at high pressures. The correlations used in the models are listed in Appendix 3. As can be seen from Figure 3 and 4, this model predicts the observed data for down flow at low pressure and at high pressure well, but not so well for up-flow especially at low pressure and high feed concentration. The reason may be due to mass transfer correlations used which may predict a lower performance (than observed experimentally) at high space times in the upflow operating mode. This model has the drawback of not considering pellet scale phenomena and has to be supplied with apparent kinetics (pellet effectiveness factor) as an input (or a fitting parameter).

Pellet scale phenomena viz. the reaction diffusion equations (as given by Beaudry et al., 1987) were used to attempt predictions both at low and high pressures. Analytical solutions of Beaudry et al. (1987) were used at low pressure, while reaction diffusion equations are solved numerically for a partially and completely wetted pellet for high pressure data. The Beaudry (1987) model predictions were also shown on the Figure 3 and 4 for low and high pressure. As can be seen, Beaudry's model predicts downflow performance exactly as El-Hisnawi's model does, and predicts upflow performance with a little difference (although some effect of mass transfer can be seen at high space times due to the correlations used). For high pressure both El-Hisnawi's and Beaudry's models predict experimental data quite well by using our intrinsic data and Langmuir-Hinshelwood rate form.

Effect of feed concentration on performance of trickle beds and upflow reactors are also plotted in Figure 5 (a) and (b). From Figure 5 (a) we can see that both models predict the same result and match experimental data for downflow well, however, upflow prediction of the two models differ (Figure 5b) which was already observed in Figure 3. It must be mentioned that the reactor scale model failed to predict experimental data at 100 psig when the reaction is neither gas limited nor liquid limited because the model assumptions were for the extreme conditions of one reactant being limiting. Pellet scale modified model should be able to cover all cases.

CONCLUSIONS

The performance of upflow and downflow is reaction system dependent i. e., whether the reaction is gas or liquid limited under the conditions of investigation. The laboratory reactors are operated in the range of partially to fully wetted catalyst to demonstrate that the influence of wetting can be detrimental or beneficial, depending upon the reactant limitation. Models that account for these two effects can predict the performance over the entire range of operating conditions.

The intrinsic kinetics of the reaction studied is different at different pressures and hence it is recommended to study slurry kinetics at the operating pressure before any scale up or modeling is attempted. A rate expression with different rate constants at different pressures can be used to predict the trickle bed reactor data well.

The predictions of the reactor scale and pellet scale models are satisfactory for current conditions although there is a need for high pressure correlation for mass transfer coefficient and interfacial area in order to predict performance with greater certainty, especially in cases where the rate is affected significantly by external mass transfer.

ACKNOWLEDGMENT

Table 1. Identification of the Limiting Reactant for Literature and Present Data.

	Reaction System	Operating conditions	Gamma (γ)	limiting reactant	Preferred mode
Goto (1984)	Oxidation of ethanol in presence of carbonate	Low concentration and atmospheric pressure	314	gas	downflow
Beaudry (1987)	Hydrogenation of alpha-methylstyrene	High concentration low pressure	92	gas	downflow
Mazzarino(1989)	I. Ethanol oxidation	Low concentration and atmospheric pressure	0.51	liquid	upflow
	II. Ethanol oxidation	High concentration and atmospheric pressure	17	gas	downflow
Goto (1993)	Oxidation of ethanol in presence of carbonate	Atmospheric pressure	10300	gas	downflow
This study	I. Hydrogenation of alpha-methylstyrene	High concentration low pressure	8.8	gas	downflow
	II. Hydrogenation of alpha-methylstyrene	Low concentration high pressure	0.87	liquid	upflow

Table 2. Operating Conditions for Upflow and Downflow Experiments

Pressure	30 - 200 psig (3 -15 atm.)
Concentration of α-methylstyrene	3.1 - 7.8 %(v/v) (230-600 mol/m^3)
Superficial Gas Velocity (Mass Velocity)	3.8 - 14.4 cm/s (3.3x10^{-3}-12.8x10^{-3} kg/m^2 s)
Superficial Liquid Velocity (Mass Velocity)	0.09-0.5 cm/s (0.63 - 3.85 kg/m^2 s)

Table 3. Slurry Rate Constants at Different Pressures

Pressure (psig)	kvs (m^{3}liq./m^{3}cat./s) *(mol/m^3 liq)$^{m'-1}$	K1	K2	β
30	0.0814	0	0	0
100	1.14	4.41	11.48	1
200	0.022	2.73x10^{-2}	2.1x10^{-2}	2

NOTATION

a_{glS}	=	Inactive liquid-solid contact area per unit reactor volume due to stagnant liquid film.
a_{lS}	=	Active liquid-solid contact area per unit reactor volume.
$C_{A,e}$	=	Equilibrium concentration of gaseous reactant in the liquid phase.
$C_{A,L}$	=	Concentration of gaseous reactant in the liquid phase.
$C_{A,LS}$	=	Concentration of gaseous reactant in the liquid phase on the catalyst surface.
$C_{A,glS}$	=	Concentration of gaseous reactant in the stagnant liquid phase on the catalyst surface.
C_A	=	Concentration of gaseous reactant in liquid phase (mol/m^3)
C'_A	=	Dimensionless concentration of A in the catalyst pellet
C_B	=	Concentration of liquid reactant in the liquid phase (mol/m^3).
C_{Bi}	=	Concentration of liquid reactant in liquid phase (mol/m^3).
C'_B	=	Dimensionless concentration of B in the catalyst pellet
C'_C	=	Dimensionless concentration of C in the catalyst pellet
D_{eA}	=	Effective diffusivity of gaseous reactant in the catalyst (m^2/s)
D_{eB}	=	Effective diffusivity of liquid reactant in the catalyst (m^2/s)
$(ka)_{GL}$	=	Volumetric gas-liquid mass transfer coefficient (1/s)
K_1	=	Adsorption equilibrium constant , m^3/mol.
K_2	=	Adsorption equilibrium constant , m^3/mol.
m'	=	Numerator order in intrinsic rate (Equation 1)
k_{LS}	=	Liquid-solid mass transfer coefficient (cm/sec).
k_{vs}	=	Rate constant based on volume of catalyst, m^3 liq./m^3. cat/s *(m^3/mol)$^{(m'-1)}$
P	=	Reactor pressure (psig)
r	=	Observed rate of reaction in slurry reactor (mol/m^3/s)
S_x	=	Catalyst external surface area (m^2)
V_p	=	Catalyst Pellet Volume (m^3)
Ug	=	Gas velocity (m/s)
x'	=	Coordinate from inactively wetted surface of the pellet slab, m.
x	=	Coordinate (dimenionless) on inactively wetted side of pellet slab. $(x=1-(x'-\omega V_s/S_x)/(1-\omega)(V_s/S_x))$
X_B	=	Liquid reactant conversion at any axial location.
y	=	Coordinate (dimensionless) on the actively wetted side of pellet slab. $(y=(x'-2V_p/S_x + V_s/S_x)/(V_s/S_x))$.
z	=	Coordinate (dimensionless)from inactively wetted side of pellet slab $z=(x'-\omega V_p/S_x)/(2V_p/S_x -\omega V_p/S_x)$
Z	=	Axial coordinate in the reactor, m.

Greek Letters

β	=	Denominator exponent for the rate equation.
δ	=	Ratio of effective diffusivities, D_{eA}/D_{eB}.
ε_B	=	Bed voidage m^3 voids/m^3 reactor.
η	=	Catalyst effectiveness factor for completely wetted pellet.
η_{CE}	=	External solid-liquid contacting effectiveness.
η_o	=	Overall effectivesness factor of pellet.
η_{ow}	=	Effectiveness factor based on completely wetted pellet.
η_{odw}	=	Effectiveness factor based on half wetted pellet.
η_{od}	=	Effectiveness factor based on completely dry pellet.
η_{ce}	=	External Contacting (wetting) efficiency.
ϕ_A	=	Thiele modulus $(V_S/S_X(k_{VS}/D_{eA})^{0.5})$.
ϕ_{We}	=	Weisz modulus, $(r_A)_{obs}(Vp/Sx)^2/(D_eC)$
ϕ'	=	Modified Thiele modulus $(V_S/S_X (k_{VS}C_A/D_{eA})^{0.5})$.
ω	=	Distance from the inactively wetted surface to the point where concentration of B goes to zero (twice the distance for the low pressure equations).
γ	=	$(D_{eB} C_{Bi})/b(D_{eA} C_A^*) \sim (D_{mB} C_B)/b(D_{mA} C_A^*)$
γ'	=	Ratio of bulk liquid concentrations, bC_A/C_B.

REFERENCES

Ahn, B. J., McCoy, B. J., and Smith, J. M., 1986, *AIChE J.* 32, No. 4, 566.

Al-Dahhan, M. H., and Dudukovic, M. P., 1995, *Chem. Eng. Sci.* 50, No. 15, 2377-2389.

Beaudry, E. G., Dudukovic, M. P., and Mills P. L., 1987, *AIChE J.* 33, No. 9, 1435.

Chen, S. Y., McCoy, B. J., and Smith, J. M., 1986, *AIChE J.* 32, No. 12, 2056.

Doraiswamy, L. K. and Sharma, M. M., Heterogeneous Reactions, Vol.I, John Wiley and Sons, New York, **1984.**

El-Hisnawi, A. A., *D.Sc. Thesis, Washington University,* St. Louis, Missouri, **1981.**

El-Hisnawi, A. A., Dudukovic, M. P., and Mills, P. L., 1982, *Am. Chem. Soc. Symp. Ser.* No 196, 421.

Germain, H., Lefebvre, A. G., and L'Homme, G. A., 1974, *ACS Monog. Ser.* 133, 164.

Goto, S.; Mabuchi, K.; 1984, *Can. J. Chem. Eng.* 62, 865-869.

Goto, S., Chatani, T., and Matouq, M. H., 1993, *Can. J. Chem. Eng.* 71, 821-823.

Harold, M.P., and Watson, P.C., *Chem. Eng. Sci.* 48, No. 5, 981-1004, 1993.

Herskowitz, M., Carbonnel, R. G., and Smith, J. M., 1979, *AIChE J.* 25, 272.

Mazzarino, I., Occhetti, M., Baldi, G., and Sicardi, S., 1989, *Chem. Eng. Comm.* 75, 225-240.

Mills, P. L. and Dudukovic, M. P., 1980, *Chem. Eng. Sci* 35, 2267.

Mills, P. L., Beaudry, E. G., and Dudukovic, M. P., 1984, *Inst. Chem. Eng. Symp. Ser.* 87, 527.

Satterfield, C. N., Ma, Y. H., and Sherwood, T. K., 1968, *Inst. Chem. Eng. Symp. Ser.* 28, 22.

Satterfield, C. N., and Roberts, G.W., 1968, *AIChE J.* 14, 159.

Wu, Y.X., and Khadilkar, M.R., 1995, CREL Annual Report,Washington University, St. Louis, USA.

Appendix 1: Governing equations for El-Hisnawi (1982) model

$$-u_{SL} \frac{dC_B}{dz} - \eta k_{vs}(1-\varepsilon_B)\eta_{CE}C_{A,LS} - \eta(1-\varepsilon_B)(1-\eta_{CE})k_{vs}C_{A,gLS} = 0$$

$$-u_{SL} \frac{dC_{A,L}}{dz} + (ka)_{gL}[C_{A,e} - C_{A,L}] - k_{LS}a_{LS}[C_{A,L} - C_{A,LS}] = 0$$

and

$$k_{LS}a_{LS}(C_{A,L} - C_{A,LS}) = \eta k_{vs}(1-\varepsilon_B)\eta_{CE}C_{A,LS}$$

$$k_{gLS}a_{gLS}(C_{A,e} - C_{A,gLS}) = \eta k_{vs}(1-\varepsilon_B)(1-\eta_{CE})C_{A,gLS}$$

Boundary conditions:

$$C_{A,L}(z)|_{z=0} = C_{A,e} \quad \text{Equilibrium feed}$$

$C_{A,L}(z)|_{z=0} = 0$ Non-Equilibrium feed

and

$C_B(z)|_{z=0} = C_{Bi}$

Model equations at high pressure (boundary conditions are the same as at low pressure)

$$-u_{SL}\frac{dC_{B,L}}{dz} - k_{LS}a_{LS}[C_{B,L} - C_{B,LS}] = 0$$

$$-u_{SL}\frac{dC_{A,L}}{dz} + (ka)_{gL}[C_{A,e} - C_{A,L}] - k_{LS}a_{LS}[C_{A,L} - C_{A,LS}] = 0$$

and

$$k_{LS}a_{LS}(C_{A,L} - C_{A,LS}) = \frac{\eta k_{vs}(1-\varepsilon_B)\eta_{CE}C_{A,LS}C_{B,LS}}{(1 + K_1C_{B,LS} + K_2C_{C,LS})^\beta}$$

$$k_{LS}a_{LS}(C_{B,L} - C_{B,LS}) = \frac{\eta k_{vs}(1-\varepsilon_B)\eta_{CE}C_{A,LS}C_{B,LS}}{(1 + K_1C_{B,LS} + K_2C_{C,LS})^\beta}$$

Appendix 2: Governing Equations for Beaudry (1987) model
Pellet Scale Equations:
a) Low Pressure (Gas Reactant Limited) with rate first order in A.

$$\frac{d^2C'_A}{dx^2} - (1-\omega)^2\phi_A^2C'_A = 0 \qquad 0 < x < 1$$

$$\frac{d^2C'_B}{dx^2} - (1-\omega)^2\delta\phi_A^2\gamma C'_A = 0 \qquad 0 < x < 1$$

$$\frac{d^2C'_A}{dy^2} - \phi_A^2C'_A = 0 \qquad 0 < y < 1$$

$$\frac{d^2C'_B}{dy^2} - \phi_A^2\delta\gamma C'_A = 0 \qquad 0 < y < 1$$

Boundary conditions:

$$\frac{dC_A}{dx}|_{x=0} = -(1-\omega)\frac{dC_A}{dy}|_{y=0} \text{ (=0 for m<1)}$$

$$C_A|_{x=0} = C_A|_{y=0} - 2(\frac{V_p}{V_s}-1)\frac{dC_A}{dy}|_{y=0} \text{ (=0 for m<1)}$$

$$\frac{dC_A}{dy}|_{y=1} = Bi_{LS,A}(C_{AL} - C_A|_{y=1})$$

$$\frac{dC_B}{dx}|_{x=0} = -\frac{1-\omega}{\omega + 1/Bi_{gS,A}}(1 - C_A|_{x=0})$$

$$\frac{dC_B}{dx}|_{x=1} = 0$$

$$C_B|_{x=1} = 0$$

$$\frac{dC_B}{dx}|_{x=0} = -(1-\omega)\frac{dC_B}{dy}|_{y=0}$$

$$C_B|_{x=0} = C_B|_{y=0} - 2(\frac{V_p}{V_s})\frac{dC_B}{dy}|_{y=0}$$

$$\frac{dC_B}{dy}|_{y=1} = Bi_{LS,B}(1 - C_B|_{y=1})$$

where $\qquad Bi = \frac{k_{vs}V_s}{D_eS_x} \qquad\qquad C_{AL} = C'_{Al}/C_A^*$

b) High Pressure (Liquid Reactant (diffusional) Limitation for Langmuir Hinshelwood rate form)

$$\frac{d^2C'_A}{dz^2} - \frac{(2-\omega)^2\phi'^2}{\delta\gamma}\frac{C'_AC'_B}{(1+K_1C_B+K_2C_C)^\beta} = 0 \qquad 0 < z < 1$$

$$\frac{d^2C'_B}{dz^2} - (2-\omega)^2\phi'^2\frac{C'_AC'_B}{(1+K_1C_B+K_2C_C)^\beta} = 0 \qquad 0 < z < 1$$

Boundary conditions:

$$\left.\frac{dC'_A}{dz}\right|_{z=1} = (2-\omega)Bi_{LS,A}(C'_{AL} - C'_A|_{z=1}) \qquad \left.\frac{dC'_A}{dz}\right|_{z=0} = 0$$

$$\left.\frac{dC'_B}{dz}\right|_{z=1} = (2-\omega)Bi_{LS,B}(C'_{BL} - C'_B|_{z=1}) \qquad \left.\frac{dC'_B}{dz}\right|_{z=0} = 0 \qquad C'_B|_{z=0} = 0$$

For both cases a) and b) above, the reactant conversion in general is given by

$$\frac{dX_B}{dZ} = \frac{b(1-\varepsilon_B)\eta_o(rate)}{C_{Bi}U_{SL}}$$

where

$$rate = k_{vs}C_A \qquad \qquad \text{(at low pressure)}$$

$$rate = \frac{k_{vs}C_A C_B}{(1+K_1 C_B + K_2 C_C)^\beta} \qquad \text{(at high pressure)}$$

and overall effectiveness factor is given by

$$\eta_o = (1-\eta_{ce})^2 \eta_{od} + 2\eta_{ce}(1-\eta_{ce})\eta_{odw} + \eta_{ce}^2 \eta_{ow}$$

Appendix 3: Correlations used in the models

Downflow correlations

$$\eta_{ce} = 1.617 Re_L^{0.146} Ga_L^{-0.0711} \qquad \text{El-Hisnawi (1982)}$$

$$\eta_{ce} = 1.104 Re_L^{0.33}\left[\frac{1+[\Delta P/Z)/\rho_L g]}{Ga_L}\right]^{1/9} \qquad \text{Al-Dahhan and Dudukovic (1995)}$$

$$k_{LS,A} = 4.25\frac{D_{mA}\varepsilon_p}{d_{pv}\eta_{CE}} Re_L^{0.48} Sc_L^{0.33} \qquad \text{Tan and Smith (1980)}$$

$$(Ka)_{GL,A} = 2\frac{D_{mA}(1-\frac{\varepsilon_L}{\varepsilon_B})}{d_{pv}^2}(\frac{S_x Re'_G}{d_{pv}d_R})^{0.2} Re_L^{'0.73} Sc_L^{0.5} \quad \text{Fukushima and Kusaka (1977)}$$

$$\varepsilon_L = \varepsilon_B[1-1.8(\frac{S_x}{d_{pv}^2})^{0.075} Re_G^{'0.06} Re_L^{'0.15}(\frac{d_{pv}}{d_R})^{0.3}] \quad \text{Fukushima and Kusaka (1977)}$$

$$k_{GS,A} = 0.4548\frac{H_A u_G}{\varepsilon_B} Re_G^{-0.4069} Sc_G^{-0.667} \qquad \text{Dwivedi and Upadhyah (1977)}$$

Upflow Correlations

$$Sh = (2.14 Re_L^{0.5} + 0.99)Sc_L^{0.33}$$

$$k_{LS} = \frac{ShD_{mA}}{d_{pv}\eta_{CE}} exp(0.48 log(100\frac{Re_G}{Re_L}) - 0.03(log(100\frac{Re_G}{Re_L}))^2 - 0.3)if \frac{Re_G}{Re_L} \geq 0.02$$

$$k_{LS} = \frac{ShD_{mA}}{d_{pv}\eta_{CE}} if \frac{Re_G}{Re_L} \prec 0.02 \qquad \text{Specchia (1978)}$$

$$k_{GL} = 0.0173(u_{SL}(\Delta P)_{GL})^{0.5}(\frac{D_{mA}}{D_{mB}})^{0.5} \qquad \text{Reiss (1967)}$$

$$(\Delta P)_{GL} = 3u_G^2 \rho_G\frac{(1-\varepsilon_B)}{d_{pv}\varepsilon_B} exp(8 - 1.12 log(Z) - 0.0769(log(Z))^2 + 0.0152(log(Z))^3$$

$$Z = Re_G^{1.167} Re_L^{-0.767}$$